This is the accepted manuscript made available via CHORUS. The article has been published as:

Diagrammatic quantum Monte Carlo study of an acoustic lattice polaron

Thomas Hahn, Naoto Nagaosa, Cesare Franchini, and Andrey S. Mishchenko

Phys. Rev. B **104**, L161111 — Published 15 October 2021

DOI: 10.1103/PhysRevB.104.L161111

Diagrammatic quantum Monte Carlo study of an acoustic lattice polaron

Thomas Hahn,[1] Naoto Nagaosa,[2,3] Cesare Franchini,[1,4] and Andrey S. Mishchenko[2]

[1] *Faculty of Physics, Center for Computational Materials Science, University of Vienna, A-1090 Vienna, Austria*
[2] *RIKEN Center for Emergent Matter Science (CEMS), 2-1 Hirosawa, Wako, Saitama, 351-0198, Japan*
[3] *Department of Applied Physics, The University of Tokyo 7-3-1 Hongo, Bunkyo-ku, Tokyo 113-8656, Japan*
[4] *Dipartimento di Fisica e Astronomia, Università di Bologna, 40127 Bologna, Italy*

We present a diagrammatic Monte Carlo study of a lattice polaron interacting with an acoustic phonon branch through the deformation potential. Weak and strong coupling regimes are separated by a self-trapping region where quantum resonance between various possible lattice deformations is seen in the ground state properties, spectral function, and optical conductivity. This study shows that the acoustic lattice polaron represents a distinct quantum object with unique features, markedly different from any previously considered polaron model. In particular, the acoustic lattice polaron exhibits an interplay between long- and short wavelength acoustic vibrations resulting in a composite phonon cloud which leads to the formation of multiple competing polaron states with a complex spectral response.

The fundamental conception of a polaron, an electron interacting with phonons and increasing its mass by dragging the accompanying phonon cloud with it, was formed long ago [1, 2]. Depending on the type of phonon involved and on the mechanism used to model the electron-phonon coupling [3–9], it is possible to distinguish between optical [10] vs. acoustic [11, 12] and lattice [13] vs. continuum [14] polarons. Optical polaron models have been studied extensively over the years. The gap in the spectrum of optical phonons makes them accessible to approximate approaches [15–17], approximation free numerical techniques [18–26], and even analytic methods [27]. On the contrary, acoustic polaron models have received much less attention. Due to their gapless phonon spectrum, many techniques, which work well for the optical case, either fail [27] or are effective only at weak coupling [28]. This lack of reference studies in the polaron literature is in contrast to the growing evidence that realistic calculations require a thorough treatment of electron-acoustic phonon interactions [29–41].

In general, a typical polaron model describes an electron interacting with a single phonon branch ($\hbar = 1$):

$$\hat{H} = \sum_{\mathbf{k}} \epsilon_{\mathbf{k}} c^\dagger_{\mathbf{k}} c_{\mathbf{k}} + \sum_{\mathbf{q}} \omega(\mathbf{q}) b^\dagger_{\mathbf{q}} b_{\mathbf{q}} + N^{-1/2} \sum_{\mathbf{k},\mathbf{q}} V(\mathbf{q},\mathbf{k})\, c^\dagger_{\mathbf{k}+\mathbf{q}} c_{\mathbf{k}} (b^\dagger_{-\mathbf{q}} + b_{\mathbf{q}})\,. \quad (1)$$

Here, the operator $c^\dagger_{\mathbf{k}}/b^\dagger_{\mathbf{q}}$ creates an electron/phonon with momentum $\mathbf{k}/\mathbf{q}$. The Hamiltonian is fully determined by the electron dispersion $\epsilon_{\mathbf{k}}$, the phonon frequency $\omega(\mathbf{q})$, and the interaction vertex $V(\mathbf{q},\mathbf{k})$. In lattice models, N specifies the number of unit cells and sums over momenta are restricted to the first Brillouin zone (BZ).

Every polaron eigenstate $|\nu,\mathbf{k}\rangle$ of Eq. (1) with energy $E_\nu(\mathbf{k})$ can be written as a linear combination of states in which an electron with momentum $\mathbf{k}-\mathbf{q}_1-\ldots-\mathbf{q}_n$ is accompanied by n phonons with momenta $\mathbf{q}_1,\ldots,\mathbf{q}_n$:

$$|\nu,\mathbf{k}\rangle = \sum_{n=0}^{\infty} \sum_{\mathbf{q}_1\ldots\mathbf{q}_n} \Theta^{\nu,\mathbf{k}}_{\mathbf{q}_1\ldots\mathbf{q}_n} c^\dagger_{\mathbf{k}-\mathbf{q}_1-\ldots-\mathbf{q}_n} b^\dagger_{\mathbf{q}_1}\ldots b^\dagger_{\mathbf{q}_n}|\emptyset\rangle\,. \quad (2)$$

$|\emptyset\rangle$ denotes the electron and phonon vacuum and $\Theta^{\nu,\mathbf{k}}_{\mathbf{q}_1\ldots\mathbf{q}_n}$ are expansion coefficients. For a fixed polaron momentum $\mathbf{k}$, we can identify the eigenstate $|\nu=0,\mathbf{k}\rangle$ with the lowest energy $E_0(\mathbf{k})$. The ground state (GS) $|0,\mathbf{k}_{\rm GS}\rangle$, which is usually located at $\mathbf{k}=\mathbf{k}_{\rm GS}=0$, has an energy $E_{\rm GS}=E_0(\mathbf{k}=\mathbf{k}_{\rm GS})$ and effective mass $m^*=(d^2E_0(\mathbf{k}_{\rm GS})/d\mathbf{k}^2)^{-1}$. The structure of the phonon cloud is described by the probabilities of finding n-phonons in the GS, $Z(n)=\sum_{\mathbf{q}_1\ldots\mathbf{q}_n}\left|\Theta^{0,\mathbf{k}=\mathbf{k}_{\rm GS}}_{\mathbf{q}_1\ldots\mathbf{q}_n}\right|^2$, and their average number $\langle N_{\rm ph}\rangle=\sum_n nZ(n)$. More information on the excited spectrum is contained in the spectral function $A_{\mathbf{k}}(\omega)=\sum_\nu \delta(\omega-E_\nu(\mathbf{k}))\,|\langle\emptyset|\,c_{\mathbf{k}}\,|\nu,\mathbf{k}\rangle|^2$, which has poles (sharp peaks) at energies of stable (metastable) states of the polaron. In addition, it can be instructive to study the zero temperature optical conductivity $\sigma_{\mathbf{k}}(\omega)=\pi(\omega V)^{-1}\sum_\nu|\langle 0,\mathbf{k}|\,j\,|\nu,\mathbf{k}\rangle|^2\,\delta(\omega+E_0(\mathbf{k})-E_\nu(\mathbf{k}))$, where V is the volume and j the charge current operator, since the symmetry selection rules for $A_{\mathbf{k}}(\omega)$ and $\sigma_{\mathbf{k}}(\omega)$ are different [17, 42]. The following discussion will be restricted to quantities calculated at $\mathbf{k}=\mathbf{k}_{\rm GS}=0$.

Optical polaron models with phonon dispersion $\omega(\mathbf{q})=\omega_0>0$ and interaction vertex $V(\mathbf{q},\mathbf{k})=V(\mathbf{q})$ are well understood. In the case of lattice models, it is common practice to quantify the electron-phonon coupling strength with a single parameter

$$\widetilde{\lambda}=\sum_{\mathbf{q}}\frac{2\,|V(\mathbf{q})|^2}{W\,\omega(\mathbf{q})}\,, \quad (3)$$

where W is the width of the electronic band. Polaron states for $\widetilde{\lambda}\ll 1$ and $\widetilde{\lambda}\gg 1$ show profound differences. In the weak coupling regime (WCR) at $\widetilde{\lambda}\ll 1$, the GS is light $m^*/m^*(\widetilde{\lambda}=0)\approx 1$ with a slightly distorted lattice $\langle N_{ph}\rangle\ll 1$ around the electron, whereas in the

strong coupling regime (SCR) at $\widetilde{\lambda} \gg 1$, the GS is heavy $m^*/m^*(\widetilde{\lambda}=0) \gg 1$ because of a large phonon cloud $\langle N_{ph}\rangle \gg 1$ surrounding the electron.

At $\widetilde{\lambda} = \widetilde{\lambda}_{\rm cr} \approx 1$, one may observe the self-trapping (ST) phenomenon. ST, as it was defined in the pioneer works [1, 43–45], refers to an apparent quantum resonance between WCR and SCR. There are two indicators for ST: (i) a two-peak structure in the phonon distribution function $Z(n)$, and (ii) a clear avoided crossing behavior of the GS and first excited state (FES) in the spectral response. These two fingerprints are very spectacular when the optical phonon frequency ω_0 is sufficiently small $\omega_0 \ll W$, but they are hardly observed at large ω_0 [46, 47].

The phonon spectrum of the acoustic polaron model dramatically changes the situation because the energy gap $\omega_0 > 0$, inherent to optical phonons, is missing and there is no *a priori* knowledge whether the Debye frequency Ω_0 of the acoustic phonon dispersion can be a good substitute. It so happened that all previous non-perturbative studies were restricted to a simplified continuum model [12, 48–52]. The electronic band in the continuum model is approximated by $\epsilon_{\mathbf{k}} = k^2/2$ while the phonon dispersion and interaction vertex are set to $\omega(\mathbf{q}) = v_s q$ and $V(\mathbf{q}) \sim \sqrt{q}$, with v_s a sound velocity [53]. A momentum cutoff $q \leq k_0$ is introduced to establish the maximal Debye frequency $\Omega_0 = v_s k_0$. Surprisingly, it was shown [12, 48, 49, 52, 54] that the WCR to SCR crossover is sharper for *larger* values of Ω_0. This is clearly opposite to what is found in optical polaron models, where the crossover is sharper for *smaller* ω_0.

With the present Letter, we fill a gap in the polaron literature by providing a reference study of an acoustic lattice polaron model using diagrammatic Monte Carlo [55–58] and stochastic optimization consistent constraints (SOCC) [56, 59, 60] analytic continuation. It should be noted that both methods are approximation free and are therefore especially suited for benchmark calculations.

We consider a three dimensional primitive cubic lattice with the usual tight binding dispersion for the electron

$$\epsilon(\mathbf{k}) = 2t \sum_{i=1}^{3} \left[1 - \cos(k_i a)\right] \ , \ -\pi \leq k_i < \pi \ , \qquad (4)$$

and an acoustic phonon spectrum due to nearest-neighbor force constants

$$\omega(\mathbf{q}) = \Omega_0 \sqrt{\sum_{i=1}^{3} \sin^2\left\{\frac{q_i a}{2}\right\}} \ , \ -\pi \leq q_i < \pi \ . \qquad (5)$$

The relevant parameters in Eqs. (4)–(5) are the electron hopping amplitude t, the lattice constant a and the Debye frequency Ω_0. Estimating the deformation potential $D = \sigma \nabla \cdot \mathbf{u}(\mathbf{r}) = \sigma \sum_{i=1}^{3} \partial u_i/\partial x_i$, as the energy proportional to the change of the unit cell volume $D \sim \sum_{i=1}^{3} \mid \mathbf{u}_i(\mathbf{r} + \hat{\mathbf{a}}_i) - \mathbf{u}_i(\mathbf{r}) \mid$, where $\hat{\mathbf{a}}_i$ is a primitive unit vector of the 3D cubic lattice and $\mathbf{u}_i(\mathbf{r}) \sim \hat{\mathbf{a}}_i \sum_{\mathbf{q}} e^{i\mathbf{q}\mathbf{r}} \left(b_q + b^{\dagger}_{-q}\right)/\sqrt{\omega(\mathbf{q})}$ is a displacement due to the acoustic phonon mode, one arrives at the interaction vertex

$$V(\mathbf{q}) = \gamma \sum_{i=1}^{3} \sin\left\{\left|\frac{q_i a}{2}\right|\right\} \left[\sum_{i=1}^{3} \sin^2\left\{\frac{q_i a}{2}\right\}\right]^{-1/4} . \qquad (6)$$

γ has the unit of energy and is related to the deformation potential constant σ via $\gamma = \sqrt{2\hbar\sigma^2/(Ma^2\Omega_0)}$, with M the ion mass. As is usually the case, we define a dimensionless coupling constant $\lambda = \gamma^2/(6\,t\,\Omega_0)$ which corresponds to $\widetilde{\lambda} \approx 2.5\,\lambda$, as follows from Eqs. (3)–(6). Henceforth, we set $\hbar = t = a = 1$.

Figures 1(a)–1(d) show the ground state properties (effective mass, energy, quasiparticle weight and average

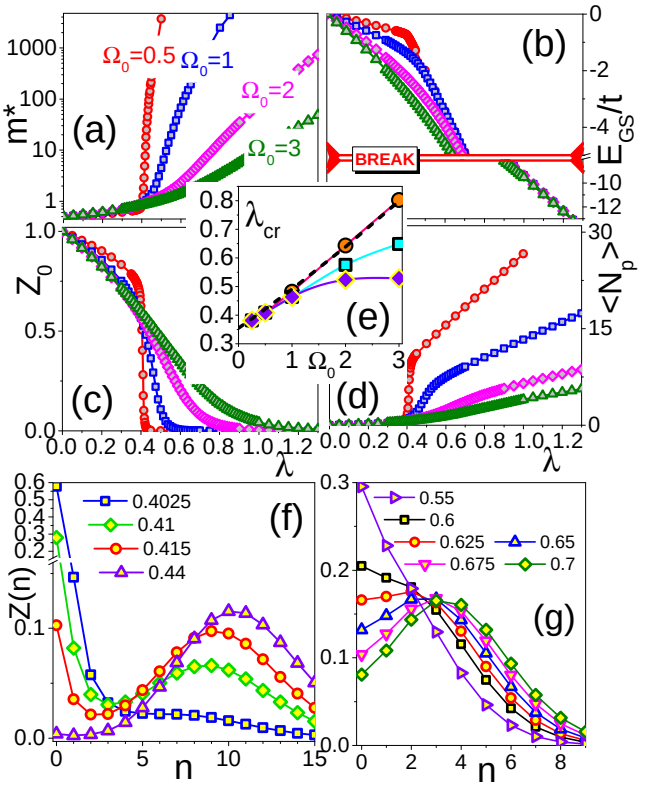


FIG. 1. (a-d) Polaron ground state properties for $\Omega_0 = 0.5$ (red circles), $\Omega_0 = 1$ (blue squares), $\Omega_0 = 2$ (magenta rhomboids), and $\Omega_0 = 3$ (olive triangles): (a) effective mass $m*$, (b) ground state energy $E_{\rm GS}$ [horizontal red double line shows a break in the y-axis from -5 to -8 separating two different energy scales], (c) quasiparticle weight Z_0, and (d) average phonon number $\langle N_{\rm ph}\rangle$ in the phonon cloud. (e) Ω_0-dependence of the critical values $\lambda_{\rm cr}$ determined from the condition $d^2 Z_0/d\lambda^2 = 0$ (rhomboids), Min$[d^2 E_{\rm GS}/d\lambda^2]$ (squares), and $d^2\langle N_{\rm ph}\rangle/d\lambda^2 = 0$ (circles). Dashed line shows extrapolation to zero Debye frequency $\Omega_0 \to 0$. (f-g) Distribution $Z(n)$ of the number n of phonons in the GS for different λ (in legend) for (f) $\Omega_0 = 0.5$ and (g) $\Omega_0 = 2$.

number of phonons) as functions of the coupling strength λ. In contrast to the acoustic continuum polaron, the transition from WCR to SCR is sharper for smaller values of the Debye energy cutoff Ω_0. This behavior is similar to what is observed in optical lattice models, where the crossover is more abrupt for smaller ratios ω_0/W. Moreover, it is interesting to note that the value of $\widetilde{\lambda}_{\rm cr} \approx 2.5\lambda_{\rm cr}$ in the adiabatic limit is in good agreement in both optical and acoustic lattice models. In Fig. 1(e), we show $\lambda_{\rm cr}(\Omega_0)$ determined from derivatives of various GS properties with respect to λ (see the caption for more details). Although the values of $\lambda_{\rm cr}(\Omega_0)$ slightly depend on the kind of derivative, this discrepancy becomes negligible at small values of Ω_0 allowing us to extrapolate to the adiabatic limit $\lambda_{\rm cr}(\Omega_0 \to 0) = 0.355 \pm 0.01$. Using Eq. (3), we can compare this value for the acoustic polaron $\widetilde{\lambda}^{\rm ac}_{\rm cr}(\Omega_0 \to 0) = 0.895 \pm 0.03$ to the one obtained for the optical polaron $\widetilde{\lambda}^{\rm op}_{\rm cr}(\Omega_0 \to 0) = 0.9$ [61, 62].

The general features of the phonon distribution function $Z(n)$ in Figs. 1(f) and 1(g) are very similar to the optical polaron case [17, 46, 63]. In the WCR, the free electron contribution to the expansion of the polaron GS in Eq. (2) is the dominant one and so $Z(n = 0) \approx 1$ while $Z(n > 0) \approx 0$. In the SCR, $Z(n)$ resembles a Poisson distribution with its mean located at $\approx 13.47\,\lambda/\Omega_0$. For the nearly adiabatic case $\Omega_0 = 0.5$ [Fig. 1(f)], $Z(n)$ develops a two-peak structure close to the critical coupling $\lambda_{\rm cr} \approx 0.41$. This self-trapping indicator is not seen in the nearly anti-adiabatic case $\Omega_0 = 2$ [Fig. 1(g)], where we always observe a single peak.

It is thus no surprise that for $\Omega_0 = 0.5$, in agreement with the resonant behavior of $Z(n)$, the spectral function in Fig. 2(a) demonstrates the avoided crossing phenomenon representative for self-trapping. At $\lambda = 0.1$, the FES is still well separated $\approx 0.2t$ from the GS, which contains nearly all of the weight, i.e. $Z_0 \approx 1$. With increasing coupling, this gap becomes smaller and the weight is slowly transferred to the FES, as can be seen from Figs. 2(b) and 2(c). At the crossover point $\lambda = \lambda_{\rm cr}$, the energy gap between GS and FES is minimal and their weights become equal.

On the other hand, it seems surprising that we can see the avoided crossing hybridization behavior for $\Omega_0 = 2$ [Figs. 2(d) and 2(e)], since there is no corresponding two-peak structure in the phonon distribution function $Z(n)$ [see Fig. 1(g)].

However, the unique feature of the acoustic lattice polaron is the presence of two distinctive groups of phonons whose properties are significantly different. Considering the dispersion in Eq. (5) and the interaction vertex in Eq. (6), one can distinguish between low momenta and energy (LME) phonons close to the Γ point and high momenta and energy (HME) phonons near the BZ boundary. We tentatively divide the phonons into LME/HME by using a sphere with radius $q_{f=1/2} = (3\pi^2)^{1/3}$, where

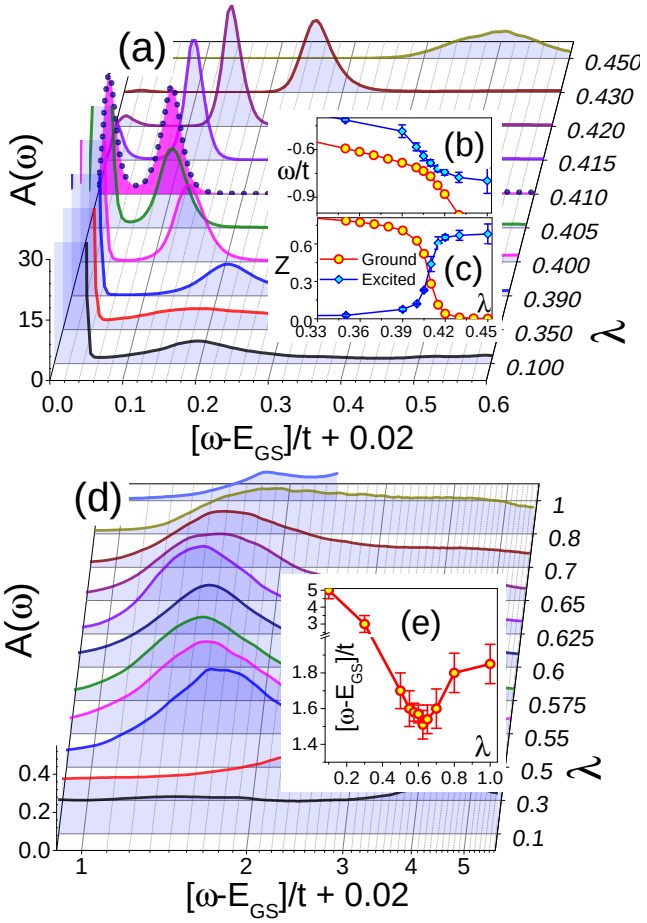


FIG. 2. (a-c) $\Omega_0 = 0.5$: (a) Spectral functions $A(\omega)/\kappa$ [κ with increasing λ is 0.006, 0.02, 0.08, 0.12, 0.23, 0.44, 0.61, 0.65, 0.67, 0.68], (b) energy, and (c) weight of the GS (red circles) and FES (blue squares) peaks. The spectrum at $\lambda_{\rm cr} \approx \lambda = 0.41$ is highlighted by a dotted line. (d-e) $\Omega_0 = 2$: (d) Incoherent part of spectral functions $A(\omega)/\kappa$ [κ with increasing λ is 0.04, 0.21, 0.45, 0.6, 0.75, 0.8, 0.8, 0.9, 0.95, 0.65, 0.2] and (e) energy of the excited state peaks counted from $E_{\rm GS}$.

f is the fraction of the volume of the BZ [see inset in Fig. 3]. Phonons with momenta inside the sphere belong to LME otherwise to HME. Figure 3 shows their different behavior for $\Omega_0 = 2$. The LME phonon cloud transfers from WCR to SCR at $\lambda \approx 0.6$, while the HME cloud makes the crossover at a considerably stronger coupling $\lambda \approx 0.725$. Depending on λ, it is thus possible to observe three qualitatively different situations in the GS: (i) LME and HME are both in the WCR, (ii) LME is in the SCR while HME is still in the WCR and (iii) LME and HME are both in the SCR. It is important to note that the number of possible GS regimes is the same as for the self-trapping phenomenon observed for optical polarons. Moreover, the situations in (i) and (iii) simply correspond to the standard WCR and SCR. However, regime (ii) is

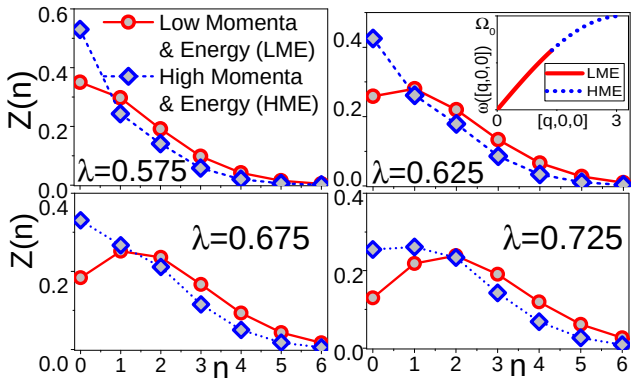


FIG. 3. Distribution of the number n of phonons in the ground state for $\Omega_0 = 2$. Phonons are grouped into LME/HME (circles/rhomboids). Inset in the upper right corner shows the division into LME and HME.

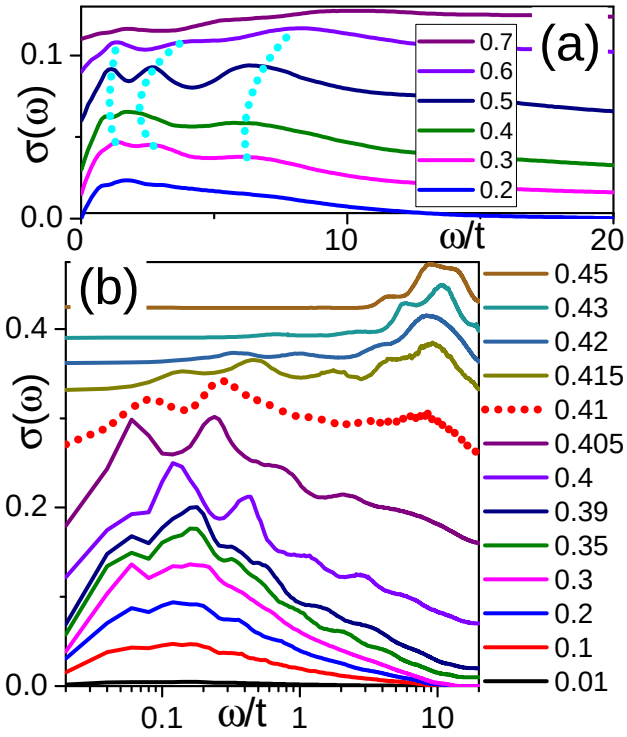


FIG. 4. Optical conductivity $\sigma(\omega) + \chi$ for different λ given in the legend. χ is an artificially added onset to discern the curves for different values of λ: (a) $\Omega_0 = 2$ [χ with increasing λ is 0, 0.015, 0.03, 0.06, 0.09, 0.11] and (b) $\Omega_0 = 0.5$ [χ with increasing λ is 0, 0, 0, 0, 0.01, 0.02, 0.07, 0.16, 0.26, 0.33, 0.36, 0.39, 0.42]. Dotted blue lines in (a) follow peaks to guide the eye. The spectrum in (b) at $\lambda_{cr} \approx \lambda = 0.41$ is highlighted by the dotted red line.

specific to the acoustic lattice polaron. It shows an additional fine structure in the LME/HME phonon clouds which is not present in the total phonon distribution $Z(n)$ [see Fig. 1(g)]. We observed no qualitative difference between LME and HME phonons for different fractions f because LME enters the SCR at smaller values of λ both for $f = 1/4$ and $f = 3/4$ (Fig. S1 and Fig. S2 in Supplementary material [64]). Besides, the LME cloud transfers for $\lambda = 0.625$ from WCR to SCR in the range $f \in [1/4, 3/4]$, whereas HME always stays in the WCR (Fig. S3 Supplementary material [64]). The configuration (iv) when LME is in the WCR and HME is in the SCR, is not seen in the GS but might be realized in some excited states. Furthermore, the very nature of acoustic phonons implies that there is always a group of soft phonons present, namely LME, which are responsible for the manifestations of the self-trapping phenomenon even for large Debye frequencies Ω_0, see Figs. 2(d) and 2(e). For $\Omega_0 = 0.5$, both LME and HME show a two-peak structure while the number of phonons n at maximal $Z(n)$ is, indeed, larger for LME (Fig. S4 in Supplementary material [64]).

The anomalously rich structure of the phonon cloud leads to the existence of multiple competing states. For example, a third competing state is clearly seen in the spectral function $A(\omega)$ for $\Omega_0 = 0.5$ (see Fig. S5 in Supplementary material [64]). To reveal more details on the excited spectrum, Fig. 4 shows the zero temperature optical conductivity (OC) $\sigma(\omega)$ calculated with approximation free SOCC. Numerous excited states, which were never observed in the OC of optical polarons, can be identified for $\Omega_0 = 2$ [Fig. 4(a)] and $\Omega_0 = 0.5$ [Fig. 4(b)]. This is a reflection of the unique composite phonon cloud of the acoustic polaron containing a combination of differently behaving LME and HME phonons. We are aware of only one pioneering variational study which investigated the optical response of the acoustic continuum polaron [65]. They used the Feynman-Hellwarth-Iddings-Platzman (FHIP) approach and identified sharp relaxed excited state (RES) peaks in the WCR to SCR crossover region. Such peaks do not develop for our lattice model but, as was shown in detail by two of the present authors in Ref. [57], a direct comparison between the FHIP and our DMC results should be done with caution.

In conclusion, we have shown that the lattice polaron interacting with an acoustic phonon branch via the deformation potential is an object whose complexity is going far beyond the previously studied optical and acoustic continuum polarons. Its most interesting feature is the existence of two groups of phonons which can interact with the quasiparticle in different ways. These two phonon clouds are responsible for the rich structure in the optical response showing multiple excited states and for the persistent self-trapping phenomenon even at large values of the Debye frequency. Furthermore, the sharpness of the crossover between weak and strong coupling has a different dependence on the Debye/cut-off frequency in the acoustic continuum polaron compared to our lattice model. Our results constitute the first com-

prehensive account of the fundamental properties of an acoustic polaron. They will be useful in detecting characteristic features of electron-acoustic phonon coupling in experiments and can further guide the exploration of polaron physics in real materials.

Acknowledgements. We are grateful to O. Barišić and S. N. Klimin for fruitful discussions. This work was supported by JST CREST Grant Number JPMJCR1874, Japan and by the joint FWO-FWF Grant No. I 2460-N36 and Grant No. I 4506. The computational results presented have been achieved in part using the Vienna Scientific Cluster (VSC).

[1] L. Landau, Phys. Zeits. d. Sowjetunion **3**, 664 (1933).
[2] S. I. Pekar, Zh. Eksp. Teor. Fiz. **16**, 341 (1946).
[3] S. Barišić, J. Labbé, and J. Friedel, Phys. Rev. Lett. **25**, 919 (1970).
[4] S. Barišić, Phys. Rev. B **5**, 932 (1972); **5**, 941 (1972).
[5] S. I. Pekar, E. I. Rashba, and V. I. Sheka, Zh. Eksp. Teor. Fiz. **76**, 251 (1979) [Sov. Phys. JETP **49**, 129 (1979)].
[6] W. P. Su, J. R. Schrieffer, and A. J. Heeger, Phys. Rev. Lett. **42**, 1698 (1979).
[7] A. Heeger, S. Kivelson, J. R. Schrieffer, and W. -P. Su, Rev. Mod. Phys. **60**, 781 (1988).
[8] D. J. J. Marchand, G. De Filippis, V. Cataudella, M. Berciu, N. Nagaosa, N. V. Prokof.ev, A. S. Mishchenko, and P. C. E. Stamp, Phys. Rev. Lett. **105**, 266605 (2010).
[9] O. Goulko, A. S. Mishchenko, N. Prokof'ev, and B. Svistunov, Phys. Rev. A **94**, 051605(R) (2016).
[10] H. Fröhlich, Advances in Physics **3**, 325 (1954).
[11] J. Bardeen and W. Shockley, Phys. Rev. **80**, 72 (1950).
[12] A. Sumi and Y. Toyozawa, J. Phys. Soc. Jpn. **35**, 137 (1973).
[13] T. Holstein, Ann. Phys. (N.Y.) **8**, 343 (1959).
[14] T. D. Lee, F. E. Low, and D. Pines, Phys. Rev. **90**, 297 (1953).
[15] M. Berciu, Phys. Rev. Lett. **97**, 036402 (2006).
[16] G. L. Goodvin and M. Berciu, Phys. Rev. B **78**, 235120 (2008).
[17] G. L. Goodvin, A. S. Mishchenko, and M. Berciu, Phys. Rev. Lett. **107**, 076403 (2011).
[18] G. Wellein and H. Fehske, Phys. Rev. B **65**, 4513 (1997).
[19] P. E. Kornilovitch, Phys. Rev. Lett. **81**, 5382 (1998).
[20] P. E. Kornilovitch, Phys. Rev. B **60**, 3237 (1999).
[21] J. Bonča, S. A. Trugman, and I. Batistić, Phys. Rev. B **60**, 1633 (1999).
[22] H. Fehske, J. Loos, and G. Wellein, Phys. Rev. B **61**, 8016 (2000).
[23] L.-C. Ku, S. A. Trugman, and J. Bonča, Phys. Rev. B **65**, 174306 (2002).
[24] P. E. Spencer, J. H. Samson, P. E. Kornilovitch, and A. S. Alexandrov, Phys. Rev. B **71**, 184310 (2005).
[25] J. P. Hague, P. E. Kornilovitch, A. S. Alexandrov, and J. H. Samson, Phys. Rev. B **73**, 054303 (2006).
[26] L. Vidmar, J. Bonča, and S. A. Trugman, Phys. Rev. B **82**, 104304 (2010).
[27] B. Gerlach and H. Löwen, Rev. Mod. Phys. **63**, 63 (1991).
[28] Z. Li, C. J. Chandler, and F. Marsiglio, Phys. Rev. B **83**, 045104 (2011).
[29] C. M. Wolfe, G. E. Stillman, and W. T. Lindley, J. Appl. Phys. **41**, 3088 (1970).
[30] S. Jeyadev and E. M. Conwell, Phys. Rev. B **35**, 6253 (1987).
[31] L. Tang, M. Long, D. Wang, and Z. Shuai, Science in China Series B-Chemistry, **52**, 1646 (2009).
[32] V. Perebeinos and P. Avouris, Phys. Rev. B **81**, 195442 (2010).
[33] K. Kaasbjerg, K. S. Thygesen, and K. W. Jacobsen, Phys. Rev. B **85**, 165440 (2012).
[34] F. Giustino, Rev. Mod. Phys. **89**, 015003 (2017).
[35] W. H. Sio, C. Verdi, S. Poncó, and F. Giustino, Phys. Rev. B **99**, 235139 (2019); W. H. Sio, C. Verdi, S. Poncó, and F. Giustino, Phys. Rev. Lett. **122**, 246403 (2019).
[36] H. Guo, W. Chu, O. V. Prezhdo, Q. Zheng, and J. Zhao, J. Phys. Chem. Lett. **12**, 3960 (2021).
[37] D. Lim, V. K. Thorsmølle, R. D. Averitt, Q. X. Jia, K. H. Ahn, M. J. Graf, S. A. Trugman, and A. J. Taylor, Phys. Rev. B **71**, 134403 (2005).
[38] P. Ruello, S. Zhang, P. Laffez, B. Perrin, and V. Gusev, Phys. Rev. B **79**, 094303 (2009).
[39] P.-A. Mante, C. C. Stoumpos, M. G. Kanatzidis and A. Yartsev, Nat. Comm. **8**:14398 (2017).
[40] B. Wu *et al.* Science Advances, **7**, eabd3160 (2021).
[41] C. Franchini, M. Reticcioli, M. Setvin, and U. Diebold, Nat. Rev. Mater. **6**, 560-586 (2021).
[42] O. Barišić, Phys. Rev. B **69**, 064302 (2004).
[43] E. I. Rashba, Self-Trapping of Excitons, in Modern Problems in Condensed Matter Sciences, Ed. by V. M. Agranovich and A. A. Maradudin, (North-Holland, Amsterdam, 1982), Vol. 2, p. 543.
[44] M. Ueta, H. Kanzaki, K. Kobayashi, Y. Toyozawa, and E. Hanamura, Exciton Processes in Solids, (Springer-Verlag, Berlin, 986).
[45] A. S. Ioselevich and E. I. Rashba, Theory of Nonradiative Trapping in Crystals, (North-Holland, Amsterdam, 1992), Vol. 34, p. 347.
[46] A. S. Mishchenko, N. Nagaosa, N. V. Prokof'ev, A. Sakamoto, and B. V. Svistunov, Phys. Rev. B **66**, 020301(R) (2002).
[47] M. Hohenadler, H. G. Evertz, and W. von der Linden, Phys. Rev. B **69**, 024301 (2004).
[48] Y. Toyozawa, Progr. Theor. Phys. **26**, 29 (1961).
[49] F. M. Peeters and J. T. Devreese, Phys. Rev. B **32**, 3515 (1985).
[50] X. Wang, Mod. Phys. Lett. B **12**, 775 (1998).
[51] R. Fantoni, Phys. Rev. B **86**, 144304 (2012).
[52] J. Vlietinck, W. Casteels, K. Van Houcke, J. Tempere, J. Ryckebusch, and J. T. Devreese, New J. Phys. **17**, 033023 (2015).
[53] G. Whitfield and P. B. Shaw, Phys. Rev. B **14**, 3346 (1976).
[54] B. M. Peeters and J. T. Devreese, Phys. Stat. Sol. (b) **119**, 219 (1982).
[55] N. V. Prokof'ev and B. V. Svistunov, Phys. Rev. Lett. **81**, 2514 (1998).
[56] A. S. Mishchenko, N. V. Prokof'ev, A. Sakamoto, and B. V. Svistunov, Phys. Rev. B **62**, 6317 (2000).
[57] A. S. Mishchenko, N. Nagaosa, N. V. Prokof'ev, A. Sakamoto, and B. V. Svistunov, Phys. Rev. Lett. **91**, 236401 (2003).
[58] T. Hahn, S. Klimin, J. Tempere, J. T. Devreese, and C. Franchini, Phys. Rev. B **97**, 134305 (2018)
[59] A. S. Mishchenko, in *Correlated Electrons: From Models*

to Materials, ed. by E. Pavarini, E. Koch, F. Anders, and M. Jarrel (Forschungszentrum Jülich GmbH, Düren 2012), pp. 14.1-4.28.
[60] O. Goulko, A. S. Mishchenko, L. Pollet, N. Prokof'ev, and B. Svistunov, Phys. Rev. B **95**, 014102 (2017).
[61] Y. Shinozuka and Y. Toyozawa, J. Phys. Soc. Jpn. **46**, 505 (1979).
[62] A. S. Mishchenko, N. Nagaosa, A. Alvermann, H. Fehske, G. De Filippis, V. Cataudella, and O. P. Sushkov, Phys. Rev. B **79**, 180301(R) (2009).
[63] A. S. Mishchenko and N. Nagaosa, Phys. Rev. Lett. **86**, 4624 (2001).
[64] Supplementary material.
[65] F. M. Peeters and J. T. Devreese, Phys. Rev. B **35**, 3745 (1987).